



Cite this: *J. Mater. Chem. A*, 2022, 10, 6475

Received 21st December 2021
Accepted 27th February 2022

DOI: 10.1039/d1ta10841g

rsc.li/materials-a

Spatiotemporal vitrimerization of a thermosetting polymer using a photo-latent catalyst for transesterification†

Jinyoung Park,^a Hyeong Yong Song,^b Subi Choi,^a Suk-kyun Ahn,^{ac} Kyu Hyun^a and Chae Bin Kim^{id} *^{ac}

Globally rising environmental concerns have increased the demand for recyclable polymers and efficient recycling practices. The lack of melt-processability of thermosets significantly limits their recycling because the simplest and most economical way to recycle polymers with a minimum carbon footprint is repairing or re-melting them into new items. To this end, an approach to spatiotemporally converting a thermoset into a processable vitrimer is presented. This was achieved by incorporating a latent, heat-stable photo-active catalyst into an otherwise thermoset, activating network exchange reactions only after light exposure and subsequent heating. The thermoset film could be repaired and/or heat-processed by simply exposing the sample to light followed by annealing at elevated temperature and pressure, whereas the repairing/heat-processing failed in the absence of the light exposure step. This approach enables the polymer to initially behave as a thermoset at all temperatures until it requires repair or heat-processing.

Polymers, including thermoplastics and thermosets, are currently one of the most widely used materials because they are inexpensive, lightweight, durable, and easily moldable for a broad range of applications. Thermoplastics can easily be melt-processed, repaired, and molded into different shapes, and therefore are recyclable. The drawbacks of thermoplastics such as low mechanical strength, poor structural integrity at elevated temperatures, and poor resistance to various organic solvents can be addressed by conventional crosslinking, yielding thermosets. However, as a consequence of crosslinking, thermosets lose their ability to flow along with melt-processability, weldability, and therefore reusability. Driven by

sharply growing environmental concerns, the demand for plastic recycling is becoming ever greater.¹ Though thermosets can be chemically and thermally recycled, the lack of melt-processability significantly limits their recycling because the simplest and most economical way to recycle polymers with the lowest carbon footprint is re-melting and reforming into new products.²

Vitrimers, a new class of polymers, have recently gained much attention not only because they behave similarly to thermosets but also owing to their thermoplastic-like properties.³ These unique characteristics of vitrimers could be realized by replacing the permanent covalent networks by dynamic bonds for crosslinking. There are many possibilities for forming dynamic networks between the polymer chains.⁴ Chains networked through non-covalent intermolecular interactions,^{5–7} reversible covalent bonds,^{8,9} and/or exchangeable covalent bonds^{10–12} enable melt-processing, recycling, and self-healing of the corresponding networked polymer. Only polymers that are crosslinked through exchangeable covalent bonds are called vitrimers. Vitrimers are more advantageous than the others because they can relax stress and even flow by triggering associative network exchange reactions while maintaining the network density. Consequently, vitrimers do not exhibit a sudden drop in viscosity upon heating, do maintain structural integrity at elevated temperatures, and remain insoluble in many organic solvents at all temperatures, while still being melt-processable and thus reusable.^{13–16}

Vitrimers can relax stress and flow through thermally activated network exchange reactions at temperatures above the topology freezing temperature (T_v).^{3,10–12} At temperatures below T_v , exchange kinetics in vitrimers become considerably slow, leading to a classical networked thermoset-like properties. Therefore, the location of T_v relative to glass transition and degradation temperatures and the network exchange kinetics above T_v are key factors governing the macroscopic melt-state properties, and thus by extension the recyclability of vitrimers. Typically, vitrimers with higher T_v behave like thermosets in a relatively wider temperature range, but with a narrower

^aSchool of Chemical Engineering, Pusan National University, Busan, 46241, Republic of Korea

^bInstitute for Environment and Energy, Pusan National University, Busan 46241, Republic of Korea

^cDepartment of Polymer Science and Engineering, Pusan National University, Busan, 46241, Republic of Korea. E-mail: cbkim@pusan.ac.kr

† Electronic supplementary information (ESI) available. See DOI: 10.1039/d1ta10841g

temperature range for melt-processing without thermal degradation. A narrow temperature range for melt-processing is especially disadvantageous because the melt viscosity of vitrimers above T_v follows the Arrhenius law, exhibiting a less reduction upon heating compared to that of thermoplastics above the glass transition temperature (T_g), which follows the Williams–Landel–Ferry (WLF) equation.¹¹ In contrast, vitrimers with lower T_v possess a wider temperature range for processing but a narrower range for being strong thermosets. Moreover, the slower network exchange kinetics of vitrimers result in poorer melt-processability and *vice versa*.

Judicious selection of catalysts for bond exchange,^{12,17} adjusting catalyst loadings,¹² or filler incorporation¹⁸ can somewhat influence the bond exchange kinetics and T_v of vitrimers. However, these efforts must be made during the preparation step; thus, it is challenging to adjust the thermomechanical properties once the vitrimer is already prepared. From a practical perspective, on-demand manipulation of bond exchange kinetics and the location of T_v of a single vitrimer is highly desirable to meet a wider range of working and processing conditions. In some studies, the photothermal effect of nanosized fillers,¹⁹ near-IR light-induced local heating,^{20,21} and light-activated bond exchange chemistries^{22–24} were explored to spatially adjust the network exchange kinetics in vitrimers. However, the bond exchange chemistries in the aforementioned studies could also be thermally activated, implying that a limited temperature range exists for vitrimers to behave as thermosets. Therefore, a particularly useful material can be realized if it behaves as a thermoset until it needs to be recycled.

To this end, a photochemical approach to spatiotemporally converting a thermoset into a vitrimer is presented. This was achieved by incorporating a latent, heat-stable photo-active catalyst into an otherwise thermosetting polymer, converting it into a vitrimer only after light exposure. A schematic describing a concept of the current work can be seen in Fig. 1. A damaged thermosetting polymer could be repaired and even heat-processed by simply exposing the sample to light followed by annealing at elevated temperature and pressure, whereas the self-healing and reprocessing failed in the absence of the light exposure step. Notably, the approach represents a spatiotemporal conversion from a thermoset to a vitrimer in a completely heat-independent manner, enabling the polymer to initially behave as a thermoset at all temperatures until it requires repair and reprocessing.

A model polymer used herein was prepared *via* thiol-Michael addition between pentaerythritol tetrakis(3-mercaptopropionate) and pentaerythritol triacrylate using benzoyl peroxide as a radical initiator (Fig. 2(a)). Thiol-Michael addition is beneficial due to its fast kinetics with high yield and insensitivity toward oxygen and water.²⁵ The molar ratio between thiol and acrylate was kept at 1 : 1. In a reactor, both monomers along with the radical initiator and triphenylsulfonium triflate (TPS) photo-acid generator (PAG) dissolved in acetone were vigorously mixed using an applicator at room temperature. The mixture was then vacuum dried at room temperature for 12 h, followed by heating at 60 °C for 3 h to yield

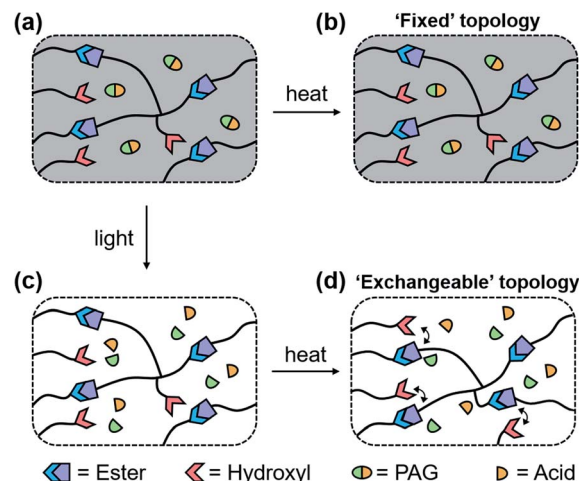


Fig. 1 A schematic describing a concept of the current work. (a) Highly networked polymer possessing a photo-acid generator (PAG) behaves as a thermoset with a 'fixed' topology. (b) Thermoset exhibits a 'fixed' topology at all temperatures. (c) Upon light exposure of the sample, acid is released from the PAG. (d) The released acid catalyzes thermally activated transesterification between hydroxyl and ester groups present in the polymer, yielding a crosslinked polymer possessing an 'exchangeable' topology.

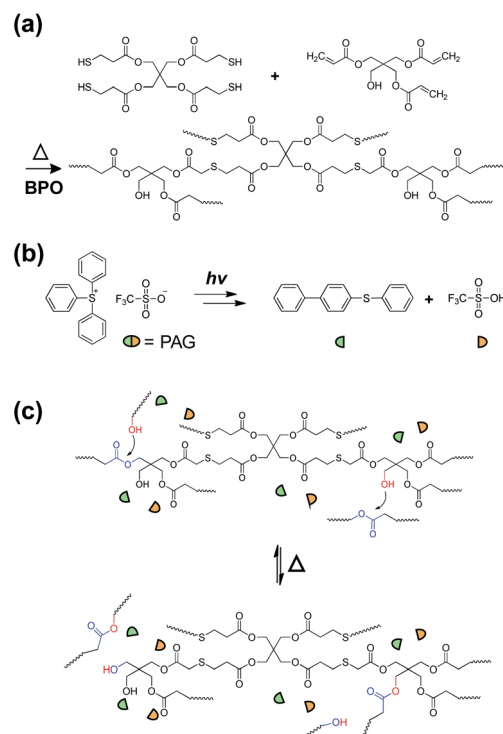


Fig. 2 (a) Synthesis of the model crosslinked polymer *via* thiol-Michael addition between pentaerythritol tetrakis(3-mercaptopropionate) and pentaerythritol triacrylate using benzoyl peroxide (BPO) as a radical initiator. (b) Schematic describing the photochemical reaction of the triphenylsulfonium triflate (TPS) photo-acid generator (PAG). (c) A schematic describing thermally activated transesterification between hydroxyl and ester groups with the aid of triflic acid.

a prepolymer. The prepolymer contained unreacted thiol and acrylate groups, as evidenced by attenuated total reflection Fourier-transform infrared spectroscopy (ATR-FTIR) (Fig. S1(a)†). The prepolymer was then fully cured and simultaneously heat-pressed into a 0.3 mm thick film at 180 °C and 15 MPa for 3 h. Curing completion upon the heat-pressing was confirmed by the disappearance of the characteristic peaks of acrylates at wavenumbers 1648–1638 cm^{-1} in the ATR-FTIR spectrum (Fig. S1(b)†). A trace peak for thiol at the wavenumber 2550 cm^{-1} was still present after heat-pressing. This fact indicates the formation of a side product such as a radical-radical termination between acrylates.²⁶ Further pressurizing the cut pieces of the film at 180 °C under 10 MPa for 3 h pulverized the sample, suggesting that the resulting crosslinked polymer film behaved as a thermoset with the lack of melt-processability (bottom row in Fig. 3(a)).

To activate the transesterification between the ester and hydroxyl groups present in the polymer, as shown in Fig. 2(c), light exposure was performed on the sample. Upon exposure to light, triflic acid was released from the incorporated TPS PAG (Fig. 2(b)). TPS PAG was chosen due to its thermal stability and commercial availability. Also, its photochemical product, triflic acid, is known to catalyze transesterification.²⁷ The thermal stability of TPS upon extensive annealing at 180 °C (the post-curing temperature for the model polymer used here) for over 4 h was confirmed by testing the pH of the TPS solution in acetonitrile using a pH indicator (Fig. S2†). Thus, a thermoset film possessing TPS could be prepared without prematurely releasing the acid.

As shown in the top row in Fig. 3(a), the light-exposed sample could be reprocessed *via* heat-pressing at 180 °C and 10 MPa for 1 h. Compared with the result shown in the bottom row in Fig. 3(a), a sharp contrast in the reprocessing was observed. This indicates that the photochemically produced acid catalyst successfully activated network exchange reactions *via* transesterification in the light-exposed polymer. To determine the light irradiation dosage, UV-vis absorption spectra of the solution with TPS and a pH indicating dye, methyl red, in an equimolar ratio in acetonitrile after various light exposure dosages were obtained (Fig. S3†). Upon increasing the irradiation dosage, the UV-vis absorbance signal near 370 nm diminished, whereas signals near 500 nm intensified. This is because protonation causes the methyl red to adopt a hydrazone structure. An exposure time longer than 2 min did not alter the absorbance further, indicating that the photochemical reaction of TPS was complete within 2 min of light exposure. Therefore, 2 min of light exposure was performed for all samples unless otherwise specified. Further UV-vis spectroscopy investigation shown in Fig. S4† revealed that a 0.3 mm thick sample with TPS exhibited 21.8% transmittance at 300 nm, which is the highest wavelength light for activating the TPS.²⁸ This fact indicates that the TPS was successfully photo-activated through the 0.3 mm thick sample. The Beer-Lambert law also predicted that the film with TPS at a thickness of 1.4 mm would exhibit 0.1% transmittance at 300 nm wavelength. Considering that the light exposure can be performed on the top and bottom surfaces of the film, we believe that the TPS can be activated through the film with a thickness up to 2.8 mm. Furthermore, it is known that small molecule diffusion in the polymer matrix takes place especially above the glass transition temperature.²⁹ This implies that thermal annealing after light exposure may result in the diffusion of the light-activated TPS beyond the light penetration depth.

A scratched sample possessing PAG self-healed when the damaged parts were exposed to light followed by annealing at elevated temperature and pressure, whereas the self-healing failed in the absence of the light exposure step (Fig. 3(b)), consistent with the reprocessing results shown in Fig. 3(a). No discernible changes in T_g , thermomechanical properties, and thermal stability were observed upon light exposure as confirmed by differential scanning calorimetry (DSC), tensile testing, dynamic mechanical analysis (DMA), and thermogravimetric analysis (TGA) as shown in Fig. 3(c)–(e) and S5,†

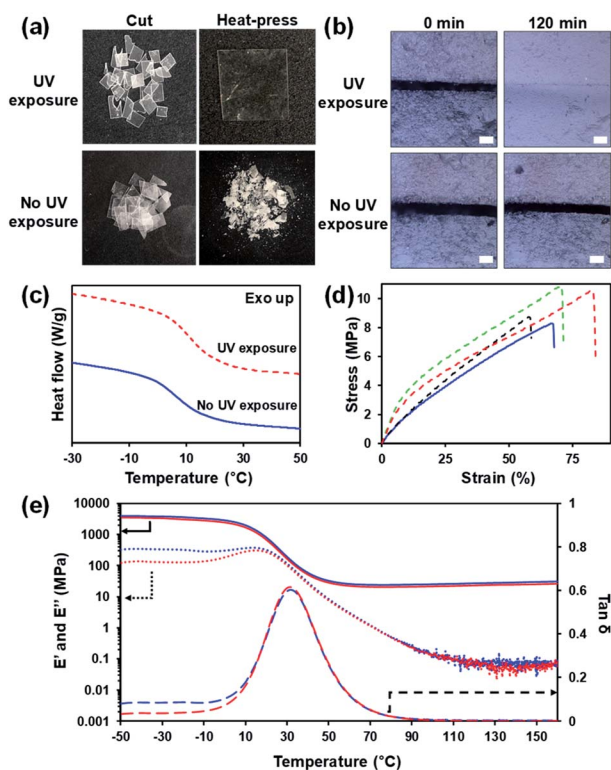


Fig. 3 (a) Melt-processability of the model polymer before (bottom) and after light exposure (top). Reprocessing was performed at 180 °C under 10 MPa for 1 h. 0.3 mm thick samples were cut with a razor blade prior to heat-pressing. (b) Optical micrographs showing self-healing for the polymer before (bottom) and after light exposure (top). Samples were heated at 180 °C. Scale bars indicate 30 μm . (c) Differential scanning calorimetry (DSC) thermograms for the light-exposed (dashed red line) and unexposed samples (blue solid line) upon second heating at a rate of 10 °C min^{-1} . Mid- T_g was determined to be 10 °C for both samples. (d) Stress–strain curves obtained for the samples at room temperature: unexposed (solid blue), light-exposed (red dashed), and reprocessed sample after light exposure (1st and 2nd generations for green and black dashed lines, respectively). (e) Dynamic mechanical analysis results for the sample before (blue) and after light exposure (red). Solid lines, dotted lines, and dashed lines represent E' , E'' , and $\tan(\delta)$, respectively.

respectively. As can be seen from Fig. 3(c) and (e), T_g values measured by DMA were higher than those characterized by DSC. Typically, the higher T_g observed in DMA is caused by a larger sample size, which causes slower heat transfer to the sample, and by the difference in measurement conditions between DSC (static conditions) and DMA (dynamic oscillation conditions). The mid- T_g measured by DSC and onset thermal degradation temperatures with 5% weight loss for the model polymer were 10 °C and 240 °C for both before and after light exposure, respectively. No other thermal transitions but T_g were observed for both unexposed and light-exposed samples as evidenced by DSC runs up to 180 °C (Fig. S6†). Notably, the light-exposed sample could be reprocessed multiple times with comparable mechanical properties (Fig. 3(d) and S7†). For both light exposed and unexposed samples, soft elastomers like mechanical properties were observed since they possessed T_g measured by DSC below room temperature.

In order to investigate the vitrimer characteristics, the linear viscoelastic properties, G' and G'' , of the model polymer were

measured. In Fig. 4(a) and (b), pseudo-master curves of unexposed and light-exposed samples were constructed at a reference temperature (T_{ref}) of 70 °C, respectively, where the plateau in G' started to appear. The time-temperature superposition shift factor (a_T) of the unexposed polymer followed the WLF relationship over the entire range of measurement temperature (Fig. 4(c)). Several studies have revealed that a_T can be well predicted by using the WLF equation for amorphous thermo-setting polymers,^{30,31} indicating that the polymer used here behaved as a thermoset before light exposure. In contrast, as shown in Fig. 4(d), the light-exposed polymer exhibited two distinct temperature dependences in a_T . At low temperatures, a_T followed the WLF behavior. However, the temperature dependence changed to the Arrhenius relationship from 80 °C. The distinct temperature dependence in a_T can be interpreted as a shift from the Rouse segmental motion dominated regime to the network exchange kinetics governed regime at 80 °C upon heating.^{32–34} Therefore, the a_T of the light-exposed polymer was fitted with the WLF equation for $T \leq 80$ °C and the Arrhenius equation for $T \geq 120$ °C. The corresponding equations and fitting parameters are listed in Table S1.†

Rheological measurements indicated that the light-exposed sample behaved as a vitrimer with a T_v of ~ 80 °C. The activation energy for the transesterification in the light-exposed polymer was calculated to be 142.7 kJ mol⁻¹ based on the Arrhenius fit (inset in Fig. 4(d)), whereas such fitting was not valid for the unexposed polymer (inset in Fig. 4(c)). The T_v for the light-exposed polymer was defined as a crossover between the WLF and Arrhenius relationships in Fig. 4(d). A recent simulation study also showed that T_v was located very close to the transition temperature determined from a_T .³⁵ In other literature, T_v was defined as the temperature at which the melt viscosity is equal to 10¹² Pa s.¹¹ Owing to the experimental difficulty in measuring such a high viscosity, T_v was estimated by extrapolating the Arrhenius fit toward lower temperatures for the light-exposed polymer. However, this extrapolation method is not valid in the Rouse segmental motion regime below 80 °C.^{36,37} Furthermore, it is difficult to expect enough chain diffusivity to activate network exchange kinetics in vitrimers at a viscosity of 10¹² Pa s. Based on this analysis, therefore, we argue that the only possible way for a vitrimer to exhibit a melt viscosity of 10¹² Pa s at T_v is when T_v is in the vicinity of T_g . For this reason, as a practical criterion, the transition temperature shown in Fig. 4(d) was used as T_v for the light-exposed polymer. As can be seen from Fig. S8,† the unexposed sample could not relax stress at 130 °C ($>T_v$). A slight stress reduction was attributed to the chain conformational changes and/or internal stress release, which are common for thermosets. On the other hand, the light exposed polymer was capable of relaxing stress due to the activated transesterification.

To highlight the versatility of our approach, a spatiotemporally controlled reshaping experiment was conducted and a schematic representation is shown in Fig. 5(a). Each step of the process was monitored and recorded, as depicted in Fig. 5(b). First, a rectangular specimen was prepared and only half of the sample was exposed to light at room temperature for 2 min. Then, the specimen was twisted twice to form a helical

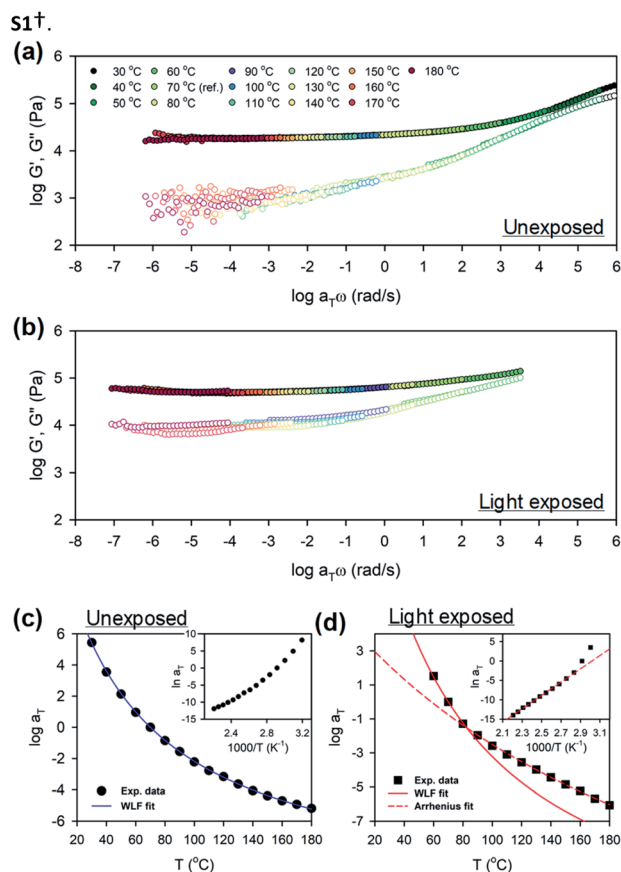


Fig. 4 Pseudo-master curves of G' (filled symbols) and G'' (unfilled symbols) at $T_{ref} = 70$ °C for the polymers containing TPS (a) before and (b) after light exposure. Horizontal shift factor a_T as a function of temperature with $T_{ref} = 70$ °C for the model polymers possessing TPS (c) before and (d) after light exposure. The solid lines indicate the WLF fit, while the dashed line indicates the Arrhenius fit. The T_v for the vitrimer was determined to be 80 °C based on the crossover between WLF and Arrhenius fits in (d). Insets in (c) and (d) are the plots of $\ln a_T$ against $1000/T$ for the model polymer before and after light exposure, respectively.

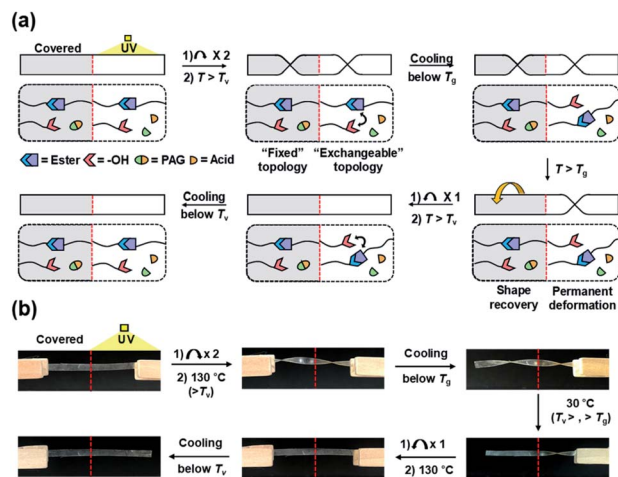


Fig. 5 (a) Schematic representation of the spatiotemporally controlled reshaping. (b) Photographs showing the reshaping experimental process.

shape, and then heated at 130 °C (> T_g or 80 °C) for 20 min, while the helical shape was fixed with clips at both ends, followed by cooling to a temperature below T_g . Then, the clip at the end of the unexposed part was removed. Upon annealing at 30 °C, which is above T_g for the unexposed part and in between T_g and T_g for the light exposed part, the unexposed (or thermoset) part spontaneously reverted to its original rectangular shape, whereas the light-exposed (or vitrimer) part maintained its twisted helical shape owing to the network rearrangement *via* transesterification. The light-exposed part could further regain its original rectangular shape by untwisting and subsequent thermal annealing at temperatures above T_g . An additional controlled reshaping (bending) test along with shape recovery comparison between the unexposed and light exposed samples can be seen from Fig. S9 and S10,[†] respectively.

Conclusions

In summary, to induce melt-processability and thus extend the reusability of a thermoset, a photochemical approach for converting a thermoset to a vitrimer is described. By incorporating a latent and heat-stable catalyst into a thermoset, photo-conversion of a thermoset into a vitrimer was successfully achieved in a completely heat-independent manner. The self-healing and reprocessing of the thermoset were realized by simply exposing the specimen to light, followed by annealing at elevated temperature and pressure, whereas those failed in the absence of the light exposure step. To further demonstrate the unique versatility toward designable on-demand shape memory polymers, a spatiotemporally controlled reshaping experiment was performed. The presented approach enabled the polymer to initially behave as a thermoset at all temperatures until it requires repair and reprocessing. As transesterification is sensitive to triflic acid generated by TPS, the method could be considered as a versatile tool and can be adopted for many other thermosets and vitrimers bearing ester and hydroxyl groups.

Conflicts of interest

There are no conflicts to declare.

Acknowledgements

This work was supported by a National Research Foundation of Korea (NRF) grant funded by the Korean government (MSIT) (2020R1C1C1003280 and 2021M3H4A1A03041403).

References

- H. Sardon and A. P. Dove, *Science*, 2018, **360**, 380–381.
- Z. O. G. Schyns and M. P. Shaver, *Macromol. Rapid Commun.*, 2021, **42**, 200415.
- M. Guerre, C. Taplan, J. M. Winne and F. E. Du Prez, *Chem. Sci.*, 2020, **11**, 4855–4870.
- W. Denissen, M. Driesbeke, R. Nicolaÿ, L. Leibler, J. M. Winne and F. E. Du Prez, *Nat. Commun.*, 2017, **8**, 14857.
- P. Cordier, F. Tournilhac, C. Soulie-Ziakovic and L. Leibler, *Nature*, 2008, **451**, 977–980.
- S. Seiffert and J. Sprakel, *Chem. Soc. Rev.*, 2012, **41**, 909–930.
- C. B. Kim, K. B. Jeong, B. J. Yang, J.-W. Song, B.-C. Ku, S. Lee, S.-K. Lee and C. Park, *Angew. Chem., Int. Ed.*, 2017, **56**, 16180–16185.
- C. N. Bowman and C. J. Kloxin, *Angew. Chem., Int. Ed.*, 2012, **51**, 4272–4274.
- C. J. Kloxin, T. F. Scott, B. J. Adzima and C. N. Bowman, *Macromolecules*, 2010, **43**, 2643–2653.
- M. Capelot, D. Montarnal, F. Tournilhac and L. Leibler, *J. Am. Chem. Soc.*, 2012, **134**, 7664–7667.
- D. Montarnal, M. Capelot, F. Tournilhac and L. Leibler, *Science*, 2011, **334**, 965–968.
- M. Capelot, M. M. Unterlass, F. Tournilhac and L. Leibler, *ACS Macro Lett.*, 2012, **1**, 789–792.
- N. Zheng, Y. Xu, Q. Zhao and T. Xie, *Chem. Rev.*, 2021, **121**, 1716–1745.
- N. J. Van Zee and R. Nicolaÿ, *Prog. Polym. Sci.*, 2020, **104**, 101233.
- Y. Yang, Y. Xu, Y. Ji and Y. Wei, *Prog. Mater. Sci.*, 2021, **120**, 100710.
- J. Zheng, Z. M. Png, S. H. Ng, G. X. Tham, E. Ye, S. S. Goh, X. J. Loh and Z. Li, *Mater. Today*, 2021, **51**, 586–625.
- J. L. Self, N. D. Dolinski, M. S. Zayas, J. R. de Alaniz and C. M. Bates, *ACS Macro Lett.*, 2018, **7**, 817–821.
- M. Goh, H. Shin and C. B. Kim, *J. Appl. Polym. Sci.*, 2020, **138**, e50079.
- Z. Wang, Z. Li, Y. Wei and Y. Ji, *Polymers*, 2018, **10**, 65.
- Y. Yang, Z. Pei, X. Zhang, L. Tao, Y. Wei and Y. Ji, *Chem. Sci.*, 2014, **5**, 3486–3492.
- Z. Feng, J. Hu, H. Zuo, N. Ning, L. Zhang, B. Yu and M. Tian, *ACS Appl. Mater. Interfaces*, 2019, **11**, 1469–1479.
- A. M. Mineo, M. E. Buck and R. Katsumata, *J. Polym. Sci.*, 2021, **59**, 2719–2729.
- C. Choi, J. L. Self, Y. Okayama, A. E. Levi, M. Gerst, J. C. Speros, C. J. Hawker, J. R. de Alaniz and C. M. Bates, *J. Am. Chem. Soc.*, 2021, **143**, 9866–9871.

- 24 D. Reisinger, S. Kaiser, E. Rossegger, W. Alabiso, B. Rieger and S. Schlögl, *Angew. Chem., Int. Ed.*, 2021, **60**, 14302–14306.
- 25 C. E. Hoyle and C. N. Bowman, *Angew. Chem., Int. Ed.*, 2010, **49**, 1540–1573.
- 26 D. P. Nair, M. Podgórski, S. Chatani, T. Gong, W. Xi, C. R. Fenoli and C. N. Bowman, *Chem. Mater.*, 2014, **26**, 724–744.
- 27 H. Lee, S. J. Kim, B. S. Ahn, W. K. Lee and H. S. Kim, *Catal. Today*, 2003, **87**, 139–144.
- 28 S. Araki, H. Ito and Y. Butsugan, *J. Org. Chem.*, 1988, **53**, 1833–1835.
- 29 C. Saller, F.-J. Kahle, T. Müller, T. Hahn, S. Tscheuschner, D. Priadko, P. Strohmriegl, H. Bässler and A. Köhler, *ACS Appl. Mater. Interfaces*, 2018, **10**, 21499–21509.
- 30 Y. He, *Thermochim. Acta*, 2005, **439**, 127–134.
- 31 A. Shundo, M. Aoki, S. Yamamoto and K. Tanaka, *Macromolecules*, 2021, **54**, 9618–9624.
- 32 S. Wu, H. Yang, S. Huang and Q. Chen, *Macromolecules*, 2020, **53**, 1180–1190.
- 33 A. Jourdain, R. Asbai, O. Anaya, M. M. Chehimi, E. Drockenmuller and D. Montarnal, *Macromolecules*, 2020, **53**, 1884–1900.
- 34 G. M. Scheutz, J. J. Lessard, M. B. Sims and B. S. Sumerlin, *J. Am. Chem. Soc.*, 2019, **141**, 16181–16196.
- 35 A. Perego and F. Khabaz, *Macromolecules*, 2020, **53**, 8406–8416.
- 36 L. E. Porath and C. M. Evans, *Macromolecules*, 2021, **54**, 4782–4791.
- 37 F. Snijkers, R. Pasquinob and A. Maffezzolia, *Soft Matter*, 2017, **13**, 258–268.